Build. Sci. Vol. 10, pp. 217–230. Pergamon Press 1975. Printed in Great Britain

Model Verification of Analogue Infiltration Predictions

R. E. BILSBORROW*
F. R. FRICKE†

A survey of current methods of calculating natural ventilation and infiltration rates showed that most design recommendations are based on the results of digital analogue studies. As the natural ventilation rate calculation methods reviewed make a number of simplifying assumptions, which have not been experimentally verified, studies have been carried out, using scale model buildings in a wind tunnel, to investigate the validity of these methods. Calculated ventilation rates were found to be up to 30% higher than the model ventilation rates.

1. INTRODUCTION

SOPHISTICATED methods of predicting infiltration rates into buildings have been developed using electrical analogues[1] and more recently, digitized versions of these[2]. These predictions are very difficult to verify in large buildings because of (i) the difficulty in determining whether air is infiltrating into the volume of interest from outside the building or from another part of the building (infiltration rates are usually measured by the decay rate of a tracer in the air), (ii) variation in atmospheric conditions, and (iii) inherent difficulties in the tracer gas method itself [e.g. (a) it is difficult to maintain an even distribution of tracer gas in a room, (b) diffusion of tracer gas will also lead to errors in values for ventilation rates].

An alternative method of verifying infiltration predictions would be to evaluate the heat loads on buildings. Provided that other heat losses can be accurately predicted then the total infiltration rate could be easily obtained. Unfortunately, the other heat loads cannot be predicted satisfactorily.

A further alternative is to use wind tunnel models. If the analogue predictions are correct then they should apply to model buildings as well as full scale ones because Reynolds numbers are not considered in the theoretical predictions (though assumed infiltration coefficients for openings are supposedly based on real window tests). It was therefore decided to compare analogue results with model results to see whether the analogue assumptions are justified.

*Building Design Partnership, Manchester, U.K.
†Architectural Science Department, University of Sydney, Australia.

2. MODEL THEORY

Model studies of naturally induced air flow patterns have been carried out previously by several authors, e.g. Smith[3], Givoni[4]. These studies have dealt, generally, with situations of the type likely to be met in tropical and sub-tropical countries where very high ventilation rates through large window openings are typical. No studies have been noted where ventilation and infiltration rates are modelled through open areas of the order of 1% of the facade area, which is more typical of the situations encountered in cool temperate climates.

In aerodynamic modelling the more significant parameters which must be considered in order to ensure similarity in the air flow patterns around the model and the full scale case are geometric similarity, the Reynolds numbers of the two flows and the blockage ratio in the model study.

When considering modelling fluid flow through small orifices, and relating these values with values in full scale cases, it would seem advantageous that the Reynolds number of the flow through the model orifices should be of the same order as that through the full scale openings also. A suitable scale dimension which may be used to determine Reynolds numbers, in cases where openings are of differing geometry, is the hydraulic radius.

$$R_h = \frac{\text{cross sectional area of opening}}{\text{length of perimeter of opening}}. \quad (1)$$

However the scale length normally used in defining Reynolds number is the equivalent diameter of the opening, which is equivalent to four times the hydraulic radius. For a long thin crack, typical of the type of orifice shape through which infiltration

or controlled ventilation will occur:

$$R_h = \frac{y \cdot L}{2(y+L)}$$

where L is the crack length,
y is the crack width,
and as in this situation $L \gg y$

$$R_h \simeq \frac{y}{2} \qquad (2)$$

Thus for a long narrow opening the Reynolds number of the flow through the opening may be represented as:

$$\mathrm{Re} \simeq \frac{2 \cdot W' \cdot y \cdot \rho}{\mu} \times 10^{-3} \qquad (3)$$

where W' is the air velocity, m/s, μ is the dynamic viscosity, Ns/m^2 and ρ is the density, kg/m^3.

The order of magnitude of maximum full scale Reynolds numbers for typical infiltration openings under normal conditions may be estimated if an infiltration coefficient is known. Assuming a maximum infiltration coefficient of 10 m^3/h/m/mm wg$^{0.6}$ (maximum value quoted by Harrison[5]) and a maximum pressure difference of 5 mm wg then the maximum infiltration rate, V, will be approximately 26 m^3/h/m length of opening. But for one metre of length of opening the flow velocity, W', may be seen to be:

$$W' = \frac{0{\cdot}28\ V}{y}$$

and substituting in equation (3)

$$\mathrm{Re} \simeq \frac{0{\cdot}56 V \rho}{\mu} \times 10^{-3}$$

$$\simeq 1000.$$

Thus the working range of Reynolds numbers for flow through full scale infiltration openings may be taken as 0–1000.

The number of factors which have some effect on the amount and pattern of ventilation or infiltration is too large to enable a comprehensive study to be made. It was therefore decided to limit the study by using one standard building form. Variation in the shape of a building is influential in the pattern of ventilation mainly because a change in shape affects the pressure patterns at the ventilation openings of the building. As this effect could be studied alternatively by varying the number and distribution of these openings and the aerodynamic properties of the windstream around the building it was thought that one standard building form would be sufficient to show these effects. The models were built so that a variable number of calibrated orifices could be used to represent the openings for ventilation in the building. Pressure tappings were introduced into one face so that the external pressure coefficients could be measured and the pressure coefficients at the positions of the ventilation openings estimated by interpolation.

A model form was chosen which had openings giving model flow Reynolds numbers of the same order as full scale. Plan dimensions of the model were 120 × 120 mm and the height was 90 mm. A range of velocities between 12·5 and 25 m/s were used in the tests. The ventilation openings in the models were sets of 1·0 and 2·5 mm dia holes.

The maximum values of volume flow rate at a pressure of 15 mm wg are approximately 0·19 m^3/h and 0·03 m^3/h for the 2·5 and 1·0 mm dia holes respectively. Thus for the 2·5 mm dia holes:

$$\mathrm{Re\ max} \simeq 1800;$$

and for the 1·0 mm dia holes:

$$\mathrm{Re\ max} \simeq 700.$$

Thus the working range of Reynolds numbers through the model openings may be taken as 0–1800 and 0–700 for the 2·5 and 1·0 mm dia holes respectively. The blockage ratio of the model was approx 3% so no blockage corrections were therefore made in the experiments.

It was also decided to attempt to design the model with the same order of porosity as is normally found in buildings with all windows nominally closed or some open for ventilation. A figure for typical building permeability for office buildings with all windows closed is given in B.R.S. Digest 119[6] as 0·01–0·05% of the face area. Opening some windows for ventilation may result in permeabilities rising to maximum values of the order of 5% of the face area. The models were tested with varying numbers of ventilation openings, the minimum number representing a porosity of approximately 0·05% of the model face area, and the maximum a figure of 0·5% of the face area.

3. WIND TUNNEL

The wind tunnel in which the tests were carried out was an open-circuit tunnel with a closed working section. The lateral dimensions of the working section were 600 × 600 mm, and its length, including the distance upstream of the model mounting position available for modification of the boundary layer, was 2·0 m. A section through the wind

tunnel may be seen in Fig. 1. Tunnel working speeds were in the range 0–25 m/s.

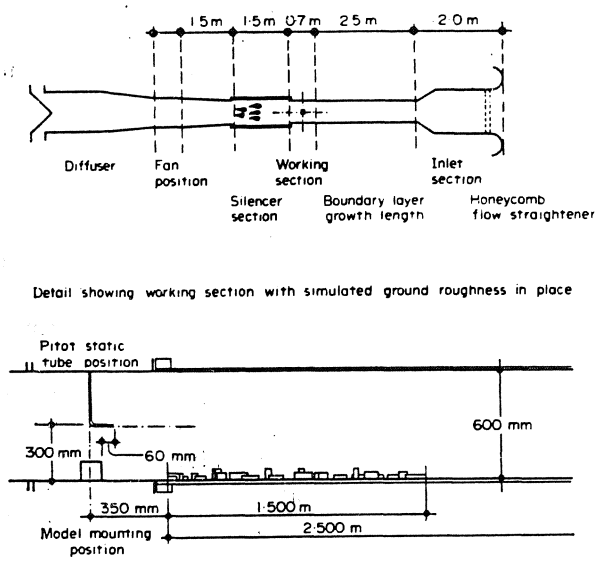

Fig. 1. Windtunnel layout.

4. VENTILATION RATE MEASUREMENT TECHNIQUES

Several techniques have been used in studies of natural ventilation and infiltration for assessing ventilation rates. The methods available and their limitations have been described by Hitchin and Wilson[7]. In most full scale studies various methods using a tracer gas have been used to indicate the mean ventilation rate in a building. In some studies measurements of air velocities have been made in order to help gain some knowledge of flow rates and patterns. These have generally been done by photographing moving flow indicators or using anemometers of various types. Model studies have also been carried out in which flow patterns have been observed by photographing moving indicators, and estimates of ventilation rates made by measuring flow velocities at finite points using hot-wire anemometers [3, 4, 8].

The full scale techniques which have been noted are not generally suitable for use in small scale model experiments. The use of tracer gas, measuring either the stable continuous concentration or the rate of decay of the tracer in a small model is difficult. In particular there are difficulties in finding a representative sampling position and in assessing the quality of mixing in the model, which would affect results. The volume of the connecting leads and analysis chamber of the gas concentration analyser is large in relation to the small volume of the model and to compensate accurately for this effect is also difficult. Finally the rate of tracer gas release required in the model would be very small and the accuracy with which this could be controlled is not likely to be high. For these reasons it was decided not to attempt to use a tracer gas ventilation rate measuring technique in the model studies.

The technique used in some previous model studies, by Givoni and others, of measuring flow velocities at discrete points in a model is also unsuitable in the present studies. Givoni measured flow velocities, using hot wire anemometers in a grid of positions in a large ($650 \times 650 \times 500$ mm) model. He used the mean velocity reading as an indication of the ventilation rate in the model. Furthermore the significance of the flow readings were corroborated using flow visualisation studies which are not possible in the present, low porosity, models, because the flow velocities are less uniform throughout the model and are much lower than in Givoni's case; mean velocities are of the order of 0·1 m/s or less for 10 m/s external speeds.

As the previous measurement techniques were not suitable for monitoring the model flow it was decided to attempt to develop alternative measuring techniques. Two types of model study were used; one in which the ventilation rate was measured directly, while in the other the pressures inside the model were measured. From both models information about the accuracy of the digital analogue technique could be inferred.

In the first set of model studies the internal pressures inside the model were studied. The digital analogue technique relies essentially on balancing the internal pressures in the building, from knowledge of the external pressures and the opening characteristics so that the net air flow into the building is equal to that leaving it. By measuring the external pressures and using calibrated openings in the model it is possible to calculate what the internal pressures should be under differing sets of conditions. By measuring the internal pressures in the model and comparing the results it is possible to get some information on the accuracy of the computer method. Consequently, it was decided to attempt to use a model which is airtight apart from the ventilation openings and in which the internal pressures may be measured.

A second set of model studies was carried out using the same model shape and orifice positions, in which flow measurements were made directly. An orifice plate mounted in a rigid diaphram was placed across the model, to measure the flow rate. In this way estimates were made of the mean volumetric flow rate through the model. The effect of the orifice plate system on the model was small because the pressure drop through the orifice system was small in relation to the pressure drop across the model. A pressure drop across the orifice

of one per cent of the pressure drop across the model leads to a reduction of flow through the model of approximately 0·5%. The system has the advantage of being simple to use and gives an accurate reading of the actual flow rate through the model rather than a deduced flow rate from velocity measurements at discrete points. The main disadvantage of this type of model is that ventilation openings may only be located in two opposite walls.

5. DESCRIPTION OF INTERNAL PRESSURE MEASUREMENT MODELS

The models used for these measurements were hollow perspex cuboids. Their dimensions were 120 × 90 mm high. The interior of each model was divided by two floors at heights of 30 and 60 mm (see Fig. 2).

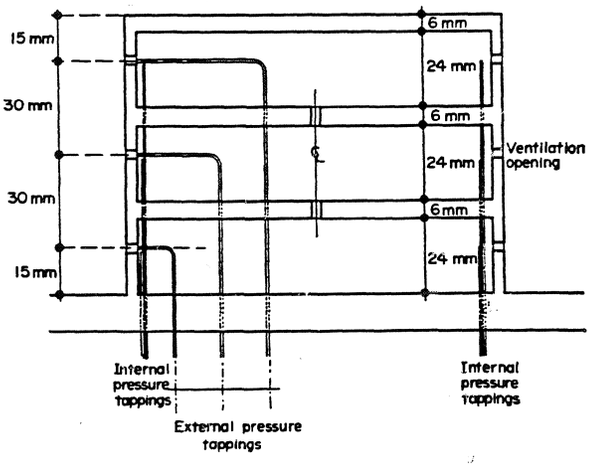

Fig. 2. Section through internal pressure measurement model.

Openings through which the model may be ventilated were made at a number of positions on each face of the model. The positions formed a square grid at centres of 30 mm. One additional opening position was located in the centre of each of the two intermediate floors in the model in order to simulate vertical flow between floors. Two ventilation opening types were used in the model tests, holes of 2·5 and 1·0 mm dia. These opening sizes were chosen to reproduce the flow characteristics of open windows and typical building infiltration passages respectively. In the models using 2·5 mm dia holes one opening was located at each grid position. In the models using 1·0 mm dia holes four openings in a square pattern, and at 2 mm centres, were located at the grid position.

On one face of each model 12 external pressure tappings were made. These tapping positions also formed a square grid at 30 mm centres; the measureing positions being established midway between the ventilation openings.

The ventilation openings used in the model tests were calibrated in a small air duct under conditions of constant flow. Pressure difference across the plate was measured using an inclined tube manometer, and flow rate was measured using a 'Gapmeter' flowmeter. The calibrations were carried out over a range of pressure differences between 2·0 mm wg pressure difference and 25·0 mm wg pressure difference, which is representative of the range of working pressures in the model tests. The calibration curves obtained for the two orifice sizes were:

For the 2·5 mm dia holes, in 3 mm thick sheet

$$V = 0{\cdot}0494\,(dP)^{1/1{\cdot}89} \tag{4}$$

and for the 1·0 mm dia holes in 3 mm thick sheet

$$V = 0{\cdot}00597\,(dP)^{1/1{\cdot}68} \tag{5}$$

The calibration is in good agreement with results calculated from Lenkei's paper[9]. The 95% confidence limits for both calibrations have values of the order of ±4% of the coefficient.

6. DESCRIPTION OF THE ORIFICE PLATE MODEL

The orifice plate chosen as being most suitable for the model ventilation rate measurements was taken from B.S. 1042. It was conical-entrance orifice plate, based on the design given in part 10 of the B.S. It is particularly suitable for measuring flow rates in viscous fluids as the coefficient of discharge remains relatively constant over a range of Reynolds numbers between 250 and 200,000.

The orifice plate was constructed in a diaphram of 6 mm perspex sheet which was placed across the ventilation model. Short settling lengths of pipe (the upstream section with a bell mouth entry), were attached to each face of the orifice plate. The orifice was positioned concentrically with the pipes. The design of the orifice plate satisfied the specification of the standard orifice plate in all respects with the exception of the lengths of the upstream and downstream settling pipe lengths. Because these pipe lengths did not meet the specification laid down, and because the orifice plate was used for a non-standard flow measuring situation the plate was independently calibrated over the working range and the results compared with the standard calibration.

The standard calibration for an orifice of this

type is given by the equation:

$$V = 0{\cdot}01252C_z\varepsilon F(D_0)^2\left(\frac{dP}{\rho}\right)^{0{\cdot}5} \quad (6)$$

where C_z is the orifice discharge coefficient, ε is the orifice expansibility factor, F is the velocity of approach factor, D_0 is the orifice plate dia, mm, D is the orifice plate pipeline dia, mm, and the Reynolds number of the flow is given by the equation:

$$\mathrm{Re} = \frac{0{\cdot}354V}{\mu D_0} \quad (7)$$

The velocity of approach factor, F, is found from the relationship:

$$F = \frac{1}{\sqrt{[1-(D_0/D)^4]}} \quad (8)$$

For the orifice geometry specified $F = 1{\cdot}005$ and found from nomograms in B.S. 1042 is 1·000 for working flow rates. The coefficient of discharge for the orifice plate is stated as 0·734 for Reynolds numbers in the range 250–5000. Using these values the standard calibration equation for the orifice plate becomes:

$$V = 2{\cdot}885\sqrt{dP} \quad (9)$$

and the expression for Reynolds number becomes:

$$\mathrm{Re} = 1276V \quad (10)$$

Thus over the working range of 0·2–3·0 m^3/h, the range of Reynolds numbers will be approx 250–4000.

Calibration of the orifice plate was carried out over the working range of flow rates with the orifice in position in the ventilation rate model. The layout of the calibration equipment is shown in Fig. 4.

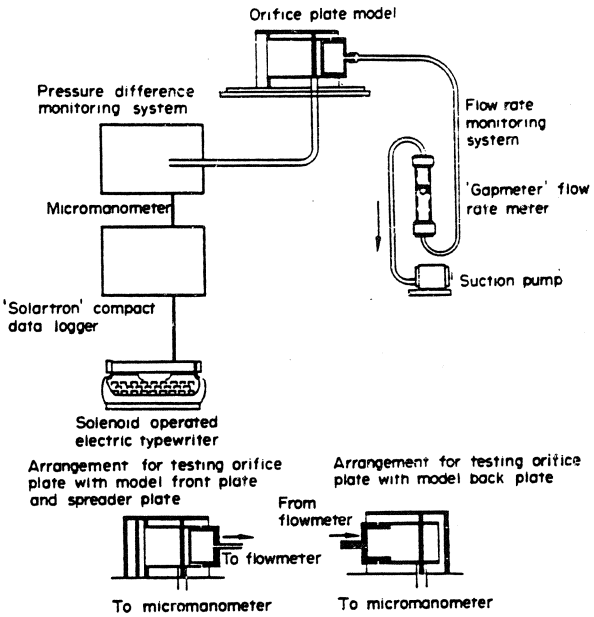

Fig. 4. Schematic layout of orifice plate calibration equipment.

A suction pump was used to provide the necessary flow rate, the flow being accurately controlled by a valve on the tube connecting it to the flow meter. The calibration of the orifice plate in the model is shown in Fig 5.

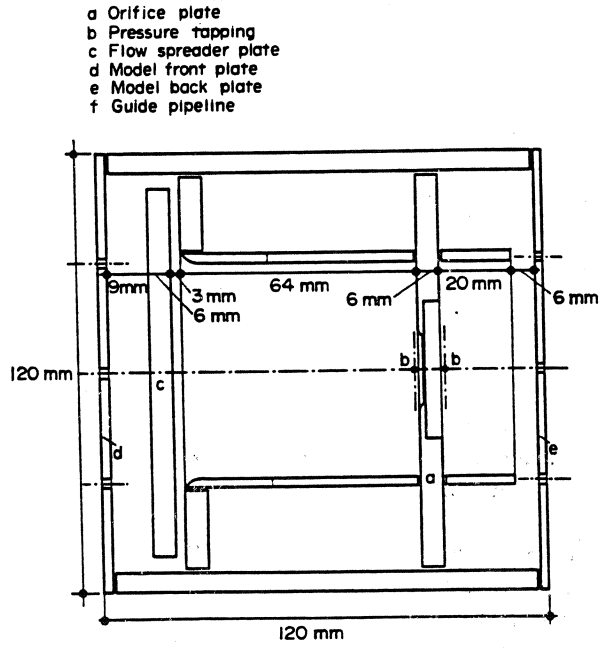

Fig. 3. Section through orifice plate model.

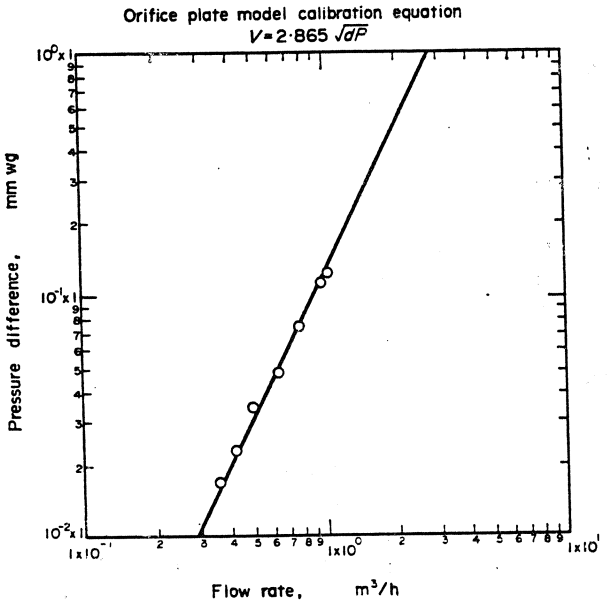

Fig. 5. Calibration of orifice plate model.

The calibration equation was of the form:

$$V = 2{\cdot}865\sqrt{dP} \qquad (11)$$

The 95% confidence limits were calculated at $\pm 0{\cdot}126\sqrt{dP}$ which corresponds to approximately $\pm 4{\cdot}5\%$ of the flow constant. This calibration was used in the model experiments with an assumed accuracy of $\pm 5\%$.

7. EXPERIMENTAL TECHNIQUE

The model experiments were carried out under two contrasting sets of flow conditions. In the initial set of experiments the model was mounted in the wind tunnel with a relatively smooth, wooden, surface upstream. This was designed to produce a boundary layer similar to the type occurring over open country. In the second set of experiments a length of considerable ground roughness was introduced which produced boundary layer conditions similar to those which might occur in urban areas. This turbulent boundary layer was developed using randomly spaced solid blocks, which extended upstream of the model for a distance of approximately 1·800 m, i.e. an isolated building was modelled. Measurements of the velocity gradients were made at the model mounting position for both sets of flow conditions, using a traversing pitot–static tube. Turbulence intensity measurements were also made at the same position using a traversing hot wire anemometer. The results of these measurements are shown in Fig. 6.

The velocity gradient measurments are in reasonable agreement with power-law gradients, the best values of the exponents being 0·14 for the simulated non-urban flow, and 0·45 for the urban flow. These values are of similar magnitude to those generally assumed for these types of flow (Davenport [10]), although the turbulence intensity values are rather lower than typical full scale values.

The internal pressure measurement models were used initially to determine the external pressure coefficients on the faces of the building. Pressure measurements were taken, at each of 12 measuring points, relative to the tunnel static pressure. Measurements were made at angles of incidence from 0 to 345° in 15° intervals, for both sets of flow conditions. Pressure coefficients for these points were calculated and pressure coefficients (based on the roof level velocity) at the ventilation opening positions obtained by interpolation.

The internal pressure measurement models were then used to measure the internal pressures inside the model under various conditions, and the results compared with calculated internal pressures. The

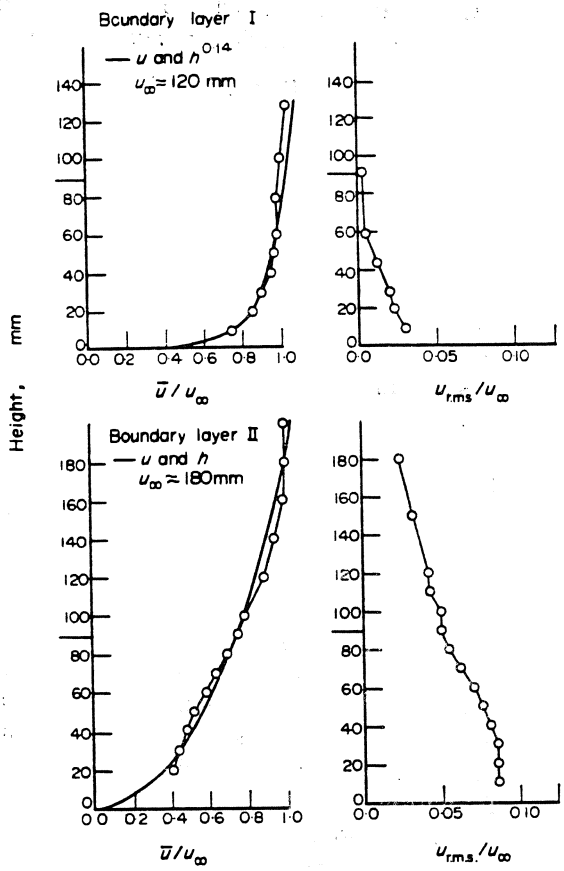

Fig. 6. Variation of velocity and turbulence intensity with height in model tests.

tests were repeated at a later time using the orifice plate model to measure the actual ventilation rates and the results again compared with the calculated ventilation rates. By using the two models in conjunction and obtaining information on both the pressure difference distributions in the models and the flow rates a much more comprehensive knowledge of the pattern of ventilation was obtained.

In all sets of measurements taken the ventilation opening areas on opposite sides of the model were nominally equal. Any difference in opening area on the sets of opposite faces would produce errors in the observed internal pressures. By turning the model through 180° and averaging the results any error of this type was negated. Similarly the models were turned to $(360-\theta)°$ and $(180-\theta)°$ in order that any effects due to the air flow direction being not parallel to the tunnel centreline might be allowed for. The internal pressure measurements, for each floor, were averaged and expressed as an internal pressure coefficient. For each set of measurements, the internal pressures were computed using the relevant air flow characteristics for the openings, and the relevant interpolated external pressure coefficients. The observed and computed pressure coefficient values were compared. The ventilation

rates were than calculated and the rates corrected to 20 m/s wind speed using the relationship:

$$V \propto (dP)^{1/n}$$

$$dP \propto (W)^2$$

$$V \propto (W)^{2/n}$$

$$\text{or } V_{20} = V_W\left(\frac{20}{W}\right)^{2/n} \tag{12}$$

For each set of measurements the volume flow rates were computed using the relevant air flow characteristics and interpolated external pressure coefficients and an assumed wind speed of 20 m/s. The observed and computed ventilation rates were then compared.

8. RESULTS AND DISCUSSION

Model ventilation studies were carried out to study the ventilation of an accurately defined set of models under closely controlled conditions, and to compare the results of the model studies with calculations using the digital analogue described by Bilsborrow[11] which is based on Jackman's[2] work. The models were used to measure either the internal pressures in the model, with respect to a reference pressure, or the mean air flow rate through the model. For each set of model observations the ventilation rate and internal pressures were calculated, using the observed external pressures, and compared with the digital analogue results.

In the initial experiments the internal pressure measurement model was used to investigate the effect of varying ventilation opening positions. Three opening distribution patterns were used: one with openings distributed uniformly over the four walls of the model, the second having a distribution pattern with two major faces (each having nine openings) and two secondary faces (each with three openings) and finally a model form with openings in two opposite faces only. More detailed studies were then made using the model with the simplest opening configuration, that is with openings in two opposite faces only. In this series of studies the air velocity, number of openings per face, opening sizes and boundary layer flow characteristics were systematically altered, and the internal pressures measured. This second set of experiments was then repeated, using the orifice plate model, and ventilation rates measured. The results of the experiments were compared with the computed figures, from which an estimate of the accuracy of the analogue technique was made.

Experimental studies were also undertaken to investigate the effect of simplifications in the input data on the accuracy of calculated ventilation rates. Two forms of data simplification were considered in this part of the work.

(a) The use of mean external pressure coefficient values for each face of the building, instead of individual values for each opening. This was investigated by repeating the comparative calculations and considering the additional errors introduced.

(b) The effect on internal ventilation rates of small scale surface features of the model, which are neglected in tables listing standard pressure coefficient values. This was done by repeating one series of model measurements with a number of small surface features attached to the major faces of the model; the range of the resulting ventilation rates being taken as an indication of the inaccuracies inherent in disregarding this aspect of design.

8.1 *Comparative model ventilation studies—experimental results*

In the initial studies carried out the effect of opening positions on the internal pressures in a porous model was studied. Internal pressures were measured and calculated for the model using different patterns of ventilation openings. Three opening patterns were used, representing a uniformly glazed building, an intermediate type and a building glazed on two opposite faces only (Fig. 7). The measurements were made in boundary layer I, using 2·5 mm diameter openings to create the porosity.

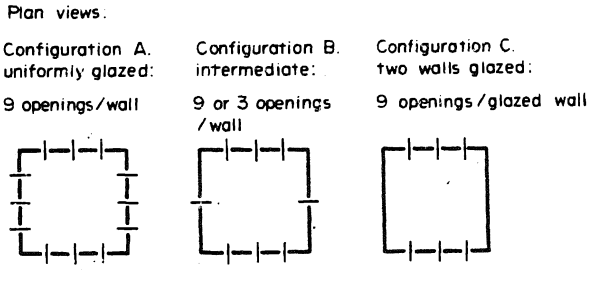

Fig. 7. Opening positions used to evaluate variation of internal pressure with opening configuration.

The variation of observed and computed values of the internal pressures with angle of incidence of the airflow for the three configurations are shown in Figs. 8–10. The internal pressures were measured separately at each level of the model, and are presented separately in the figures. The variation of internal pressures between floors of the model, in any set of conditions, was relatively small, being normally less than 0·05 of the dynamic head of the flow. The variation in computed and ob-

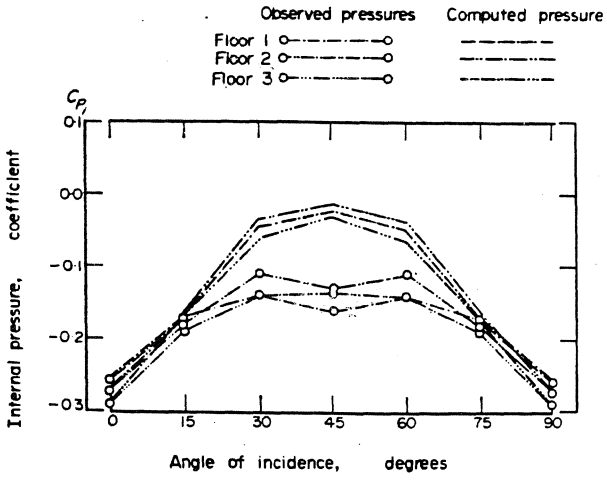

Fig. 8. Observed and computed internal pressures, opening configuration A, boundary layer I, variation with angle of incidence.

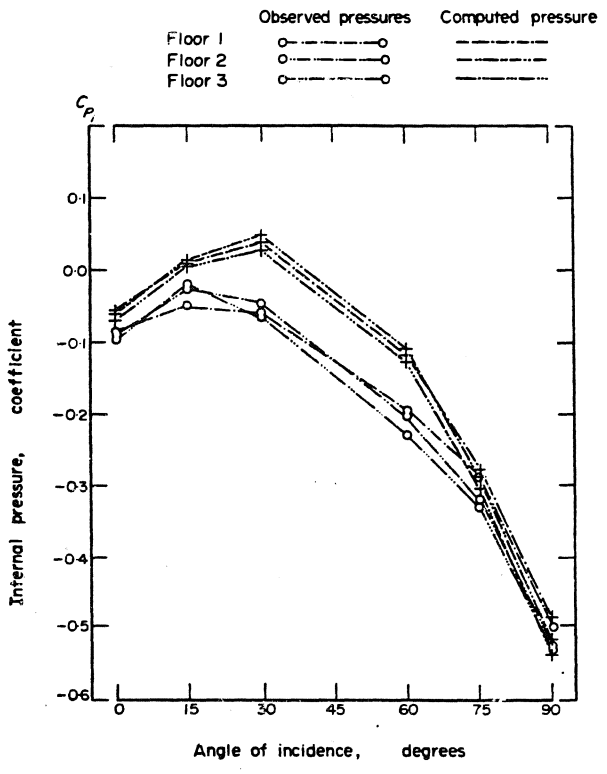

Fig. 9. Observed and computed internal pressures, opening configuration B, boundary layer I, variation with angle of incidence.

served values on the separate levels could not be compared accurately as the relevant internal resistances in the model could not be simulated exactly in the programme, which assumed the presence of an internal stairwell. Consequently, comparisons were made between the mean observed internal pressures and corresponding mean computed internal pressures.

Variations of mean internal pressure occurred with changes in distribution of the porosity in the

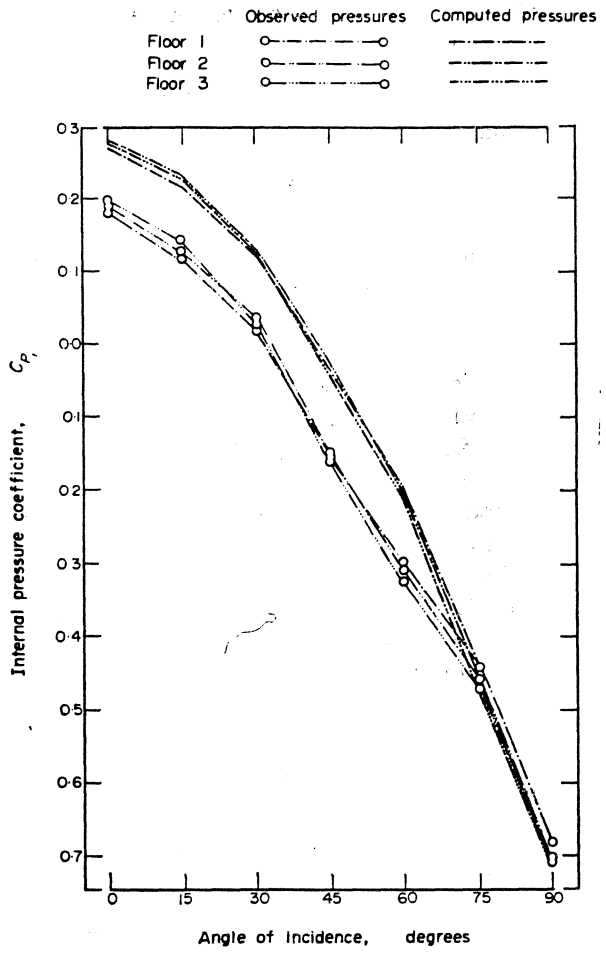

Fig. 10. Observed and computed internal pressures, opening configuration C, boundary layer I, variation with angle of incidence.

three cases. In all three cases there were significant differences between the observed and computed mean internal pressures at certain angles of incidence. In the simplest case, opening configuration C (Fig. 10), the observed pressure was significantly lower than the computed pressure at angles of incidence from 0 to 60°. The differences between the observed and computed values became much smaller at angles of incidence of 75 and 90°. These angles corresponded to those at which the mean pressure on the windward face of the model had become negative.

Measurements were also made using openings on two opposite faces of the model, both with equal and unequal porosities on the faces. The results showed very similar trends to those in Figs. 8–10. Comparative analyses of the results were carried out by calculating and plotting, for each set of results the ratio of mean pressure drop across the windward openings to mean pressure drop across the leeward openings. This expression may be used as an indication of the relative efficiency of operation of the openings in the windward and leeward

faces of the model, as is noted below:

flow into model,

$$V_1 = mCe_w(C\bar{p}_w - C\bar{p}_i)^{1/n}Pv \qquad (12)$$

and flow out of model,

$$V_2 = mCe_1(C\bar{p}_i - C\bar{p}_1)^{1/n}Pv \qquad (13)$$

where V is the volume flow rate, m^3/h, m is the number of openings/model face, C is the calibrated opening flow coefficient, $m^3/h/mm$ wg, e_w is the mean efficiency of operation of the openings in the windward face, e_1 is the mean efficiency of operation of the openings in the leeward face, $C\bar{p}_w$ is the mean external pressure coefficient acting outside the openings in the windward face of the model, $C\bar{p}_i$ is the mean model internal pressure coefficient, Cp_1 is the mean external pressure coefficient acting outside the openings in the leeward face of the model, Pv is the dynamic head of the air flow at the reference position, mm wg, and as the net flow into the model is zero:

$$mCe_w(C\bar{p}_w - C\bar{p}_i)^{1/n}Pv = mCe_1(C\bar{p}_i - C\bar{p}_1)^{1/n}Pv$$

or

$$\frac{e_w}{e_1} = \frac{C\bar{p}_i - C\bar{p}_1{}^{1/n}}{C\bar{p}_w - C\bar{p}_i}. \qquad (14)$$

The results showing the effect of change in wind speed or porosity on the relative operating efficiences of the openings, analysed by this method, are shown in Fig. 11. The pressure difference ratios calculated from the observed internal pressures followed similar patterns for the five sets of results at angles of incidence between 0 and 60°, the mean value of the ratio being approximately 1·43 at 0° and reaching a maximum value of approximately 1·80 at 45 and 60°. The value of the pressure difference ratio for the computed results varied between 1·01 and 1·03 over this range of angles of incidence. At an angle of incidence of 75° the results showed a considerably wider degree of variation. The pressure difference ratios observed for the model with nine openings per face stayed at high values while the values observed in the models with reduced porosity decreased in value. This difference was thought to have been caused because, at this angle of incidence, three of the nine openings, in the windward face of the model with full porosity, acted as air outlets so that the number of inlets and outlets became unequal and consequently the pressure difference ratio was distorted. This pattern of behaviour was confirmed by flow visualisation. If allowance is made for this change in behaviour in the most porous model, the real relative orifice operating efficiency at this angle can be shown to increase significantly, as happened in the other cases.

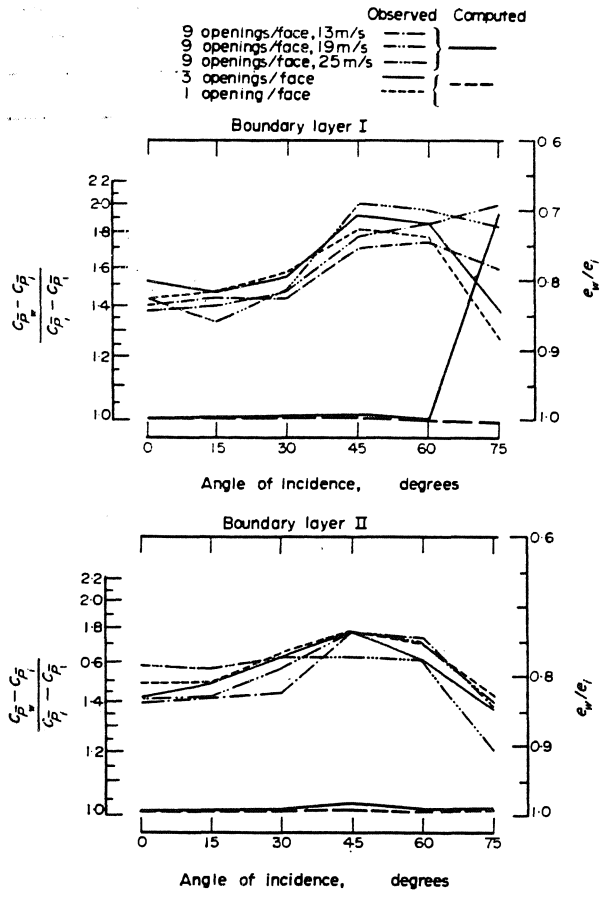

Fig. 11. Variation of pressure difference ratio $(C\bar{p}_w - C\bar{p}_1)/(C\bar{p}_i - C\bar{p}_e)$ *and relative operating efficiency* e_w/e_1, *with angle of incidence (2·5 mm openings).*

The observations of the variation of mean internal pressure with angle of incidence were also repeated in boundary layer II, using the same opening configurations and sizes. In these cases the variation of both computed and observed internal pressures with angle of incidence was much smaller due to sheltering effect of the velocity profile. The discrepancies between the observed results and the computed results followed similar patterns to those seen in the results obtained in boundary layer I.

The pressure difference ratio increased in value from approx 1·45 at 0° to a maximum of approx 1·76 at 45° and reducing in value to about 1·38 at 75° in this case.

The observations were finally repeated in both boundary layers and using the same opening configurations with a second model in which 1·0 mm dia openings were used to form the ventilating openings. The observed and computed internal pressures showed similar discrepancies to those observed in earlier tests, although the magnitude of the differences was much less. This effect may be seen clearly in the values of the pressure difference ratios which ranged between 1·14 and 1·58 for the results measured in boundary layer I and 1·12 and 1·39 for the results measured in boundary layer II.

8.2 *Orifice plate model results*

In the second part of the comparative studies the orifice plate model was used to measure ventilation rates under similar conditions to those which had been used in the previous studies. Measurements and comparative calculations were carried out using 9 or 15 2·5 mm dia openings per face and 36 or 60 1·0 mm dia openings per face on the opposite faces of the model. Measurements were made in the two boundary layers used in the previous section of the study. (The observed and computed ventilation rates are presented in Fig. 12

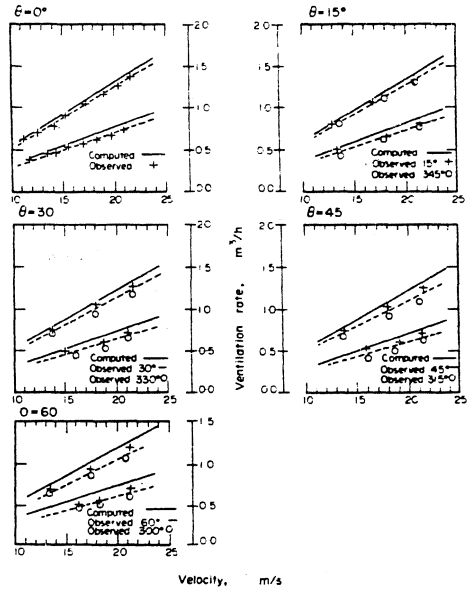

Fig. 12. Variation of observed and computed ventilation rates with air velocity, opening configuration C, 36 and 60 × 1·0 mm dia openings per face, boundary layer II.

for the 1 mm dia hole in boundary layer II.) For each set of conditions ventilation rates were measured at several wind speeds, and the observed rates corrected to a 20 m/s. wind speed. The mean observed ventilation rate, corrected to 20 m/s. wind speed was calculated and compared to the computed rate. These results are summarised in Tables 1 and 2.

The observed ventilation rates measured in boundary layer I, using the model with 2·5 mm dia openings to produce the ventilation, showed significant differences from the corresponding computed ventilation rates. At all angles of incidence the observed ventilation rates were lower than the computed rates. The mean observed ventilation rates, corrected to a 20 m/s. wind speed, at an angle of incidence of 0° were 2·66 and 1·60 m^3/h for 15 and 9 openings per face respectively. These corresponded to computed ventilation rates of 2·86 and 1·70 m^3/h, and represented 94 and 93% of the

Table 1. Computed and mean observed ventilation rates for a 20 m/s wind speed, 2·5 mm dia openings

Angle of Incidence	Computed Ventilation Rate, m^3/hr.	Observed Ventilation Rate, m^3/hr.	Standard Deviation of Observed Rates, m^3/hr.
Boundary layer I			
15 openings/face			
0°	2.86	2.66	0.04
15°	2.92	2.66	0.05
30°	2.78	2.38	0.06
45°	2.61	2.15	0.09
60°	2.31	1.88	0.04
75°	1.51	1.38	0.03
9 openings/face			
0°	1.70	1.60	0.02
15°	1.74	1.62	0.02
30°	1.66	1.50	0.02
45°	1.56	1.37	0.05
60°	1.38	1.19	0.02
75°	0.80	0.70	0.07
Boundary layer II			
15 openings/face			
0°	2.31	1.98	0.03
15°	2.31	1.96	0.05
30°	2.23	1.77	0.08
45°	2.19	1.63	0.09
60°	2.14	1.55	0.05
9 openings/face			
0°	1.37	1.19	0.03
15°	1.37	1.17	0.03
30°	1.33	1.08	0.06
45°	1.31	0.97	0.07
60°	1.28	0.94	0.03

computed rates. The observed ventilation rates showed increasing differences from the computed ventilation rates as the angle of incidence increased, reaching a maximum value at 60°, where the observed rates represented approximately 84% of the computed rates. The discrepancy decreased at an angle of incidence of 75°, where the observed rate represented about 89% of the computed rate. Mean observed ventilation rates, expressed as proportions of the computed flow rates, are summarised for all sets of model conditions in Figs. 13 and 14.

The observed ventilation rates measured in boundary layer II, using the model with 2·5 mm dia openings, show similar behaviour to those measured in boundary layer I. The discrepancies were in all cases relatively larger than those measured in boundary layer I. The observations were also repeated in the two boundary layers using 1·0 mm dia openings. The observed ventilation rates in both sets of conditions were lower than the computed rates, but the discrepancies between the respective values were in these cases considerably smaller.

Table 2. Computed and mean observed ventilation rates for a 20 m/s wind speed, 1·0 mm dia openings

Angle of Incidence	Computed Ventilation Rate, m^3/hr.	Observed Ventilation Rate, m^3/hr.	Standard Deviation of Observed Rates, m^3/hr.
Boundary layer I			
60 openings/face			
0°	1.68	1.64	0.03
15°	1.68	1.65	0.02
30°	1.59	1.58	0.06
45°	1.48	1.45	0.06
60°	1.29	1.26	0.05
36 openings/face			
0°	0.98	0.96	0.03
15°	1.00	0.99	0.04
30°	0.95	0.94	0.02
45°	0.88	0.85	0.04
60°	0.77	0.75	0.02
Boundary layer II			
60 openings/face			
0°	1.29	1.23	0.04
15°	1.29	1.23	0.03
30°	1.24	1.13	0.04
45°	1.22	1.09	0.06
60°	1.18	1.05	0.04
36 openings/face			
0°	0.76	0.70	0.03
15°	0.77	0.68	0.04
30°	0.74	0.63	0.04
45°	0.72	0.63	0.06
60°	0.70	0.59	0.03

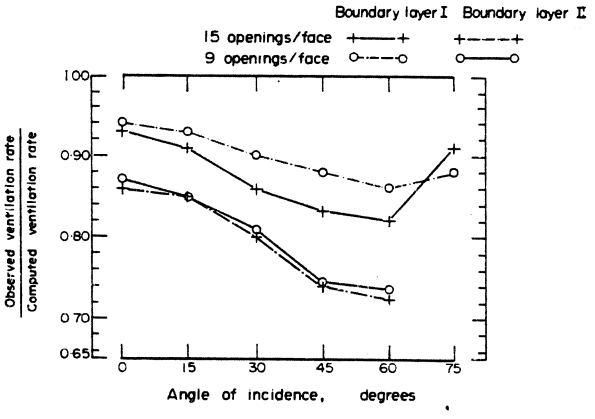

Fig. 13. Variation of relative ventilation rate with angle of incidence, 2·5 mm openings.

8.3 *Discussion*

Both the ventilation rates and the internal pressures measured in the model tests showed significant differences from the computed results. The measured internal pressures were in most cases lower than the computed values, indicating that a

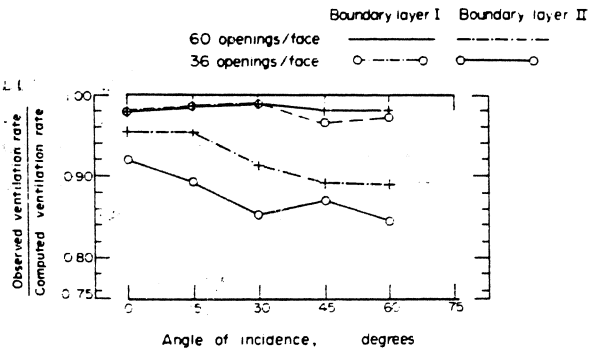

Fig. 14. Variation of relative ventilation rate with angle of incidence, 1·00 mm openings.

larger proportion of the total pressure difference acting across the model acted across the windward wall of the model than acted across the leeward face of the model. The measured ventilation rates were lower than the corresponding computed ventilation rates. The results from the two sets of observations appeared to be related to each other, as the magnitudes of both discrepancies followed similar patterns with variation of angle of incidence of the airflow and ventilation opening size.

By combining the data describing the pressure difference distributions on the windward and leeward model faces and the model ventilation rates, estimates of the operating efficiencies of the openings in these faces of the model were made. These estimated values are presented in Table 3. The analysis suggested that the openings in the leeward face of the model operated near to their calibrated efficiencies in all the model tests, whereas the openings in the windward face operated at signifi-

Table 3. Mean estimated operating efficiencies of windwardand leeward face openings, from pressure difference ratios and ventilation rates measured in model tests

	Orifice efficiency as a proportion of calibrated value				
Angle of incidence	0°	15°	30°	45°	60°
2.5 mm. diameter openings, boundary layer I					
windward face	0.86	0.84	0.82	0.74	0.73
leeward face	1.04	1.02	1.01	1.02	1.01
2.5 mm. diameter openings, boundary layer II					
windward face	0.79	0.78	0.73	0.65	0.66
leeward face	0.96	0.95	0.93	0.88	0.87
1.0 mm. diameter openings, boundary layer I					
windward face	0.92	0.92	0.92	0.87	0.88
leeward face	1.06	1.08	1.07	1.08	1.09
1.0 mm. diameter openings, boundary layer II					
windward face	0.86	0.82	0.80	0.81	0.81
leeward face	0.99	0.96	0.95	0.94	0.94

cantly lower efficiencies than the calibrated values. Three possible causes were considered in attempting to explain this behaviour.

(a) Variation of external pressure distributions over the model faces due to the presence of pressure "sinks" adjacent to the openings.
(b) Reductions in orifice efficiency due to fluctuations in the pressures acting across the openings.
(c) Reductions in orifice efficiency caused by lateral flow over the model surfaces.

The presence of pressure "sinks" adjacent to openings acting as air inlets has been described by Lawson[12]. The effect of air inlets in a plane surface is to cause variation in pressure over the surface, pressures becoming locally much lower than the mean pressure at very small distances from the openings. Due to this effect the pressure differences acting across openings will normally be lower than would be indicated from the mean pressure measured over the surface. This phenomenon was not considered to be a significant source of error, because the openings used were calibrated with reference to pressure differences measured at relatively large distances from the openings, and this procedure was repeated in the model measurements.

The effect of fluctuations in mean pressure difference on the efficiency of operation of openings is difficult to assess accurately and is normally ignored when calculating natural ventilation, as external pressures are assumed to be static. Significant pressure fluctuations did occur in the model studies, due to variations in the speed and direction of the airflow and to eddy shedding from the model. In order to establish the significance of these fluctuations a simple analysis was carried out. Assuming that sinusoidal variations in pressure took place across the openings, integrated flow rates through the openings were computed. No allowances were made for inertial effects, the frequency distribution, or waveform of the pressure fluctuations, and consequently this analysis could only be considered as a very crude estimate of the order of magnitude of these effects. The results suggested that the opening efficiencies reduced considerably as the pressure fluctuations increased in value. Measurements of the r.m.s. pressures acting on the model were also made, using a "Scanivalve" pressure transducer. Values of the r.m.s. pressures measured are shown in Fig. 15. From these measurements estimates of the reduction in operating efficiency of the openings due to this effect were made.

The reductions in efficiency of both the 1·0 and the 2·5 mm dia openings due to the pressure

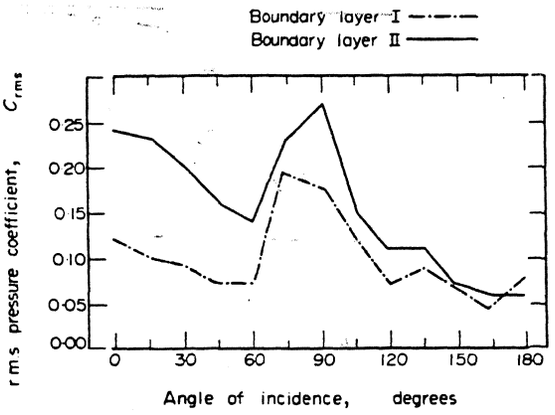

Fig. 15. Variation of RMS pressure coefficient with angle of incidence.

fluctuations measured in boundary layer I were estimated to be very small. At most angles of incidence it was estimated that the efficiency of the openings would have been between 0·98 and 1·00 of their calibrated efficiencies. The largest reductions in efficiency would have been at angles of incidence between 75 and 105°, and at these angles the openings would have been operating at efficiencies of approximately 0·95 of the calibrated value. The reductions in efficiency due to the pressure fluctuations measured in boundary layer II were larger; the windward face varied between 0·91 and 0° and 0·96 at 60°. Thus it seems unlikely that the pressure fluctuations are the main cause of the discrepancies between the observed and computed results.

The third possible explanation of the experimental results which was considered was the alteration of the opening performance due to air streams flowing laterally across the openings. The effect of lateral air movement on the performance of the openings used in the model tests was determined experimentally by repeating the calibration measurements for the openings with an air stream, of known velocity, flowing past the calibration plate. Calibration measurements were made with no lateral flow and then in several flows of different velocity. The efficiencies of operation of the openings, when acting as air inlets, were significantly lower than the calibrated values, and decreased as the lateral flow velocity increased. It was found that the efficiency could be related to the ratio of the pressure difference acting across the opening to the dynamic head of the lateral flow, as shown in Fig. 16. The measurements were repeated with the openings acting as outlets. Under these conditions the efficiencies did not appear to be significantly affected by the lateral flow.

Estimates of the influence of this effect on the observed results were made by measuring the lateral flow velocities around the model and

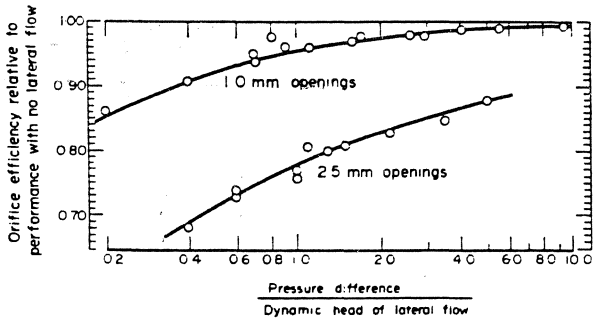

Fig. 16. Variation of orifice operating efficiency with lateral flow velocity.

calculating the reduction in efficiency of the openings in the windward model faces. The velocities found, although not necessarily accurately representative of the flow conditions over the whole face, gave approximate values of the lateral flow velocities. The reductions in estimated efficiency due to this cause followed much more closely the pattern seen in the observed results. The 2·5 mm dia openings were affected to a much greater extent than the 1·0 mm dia openings. It is thought that this effect occurred because the air supply for the 1 mm holes is drawn from the air much nearer to the model surface, where the flow rate is lower due to a boundary layer effect caused by the model surface. The reductions were also larger for the observations made in boundary layer II, due to the higher lateral flow velocities relative to the pressure differences acting across the model. The size of the correction also increased as the angle of incidence increased, the maximum value being, for both boundary layers, at an angle of 60°. The correction was lower at the angle of 75° due to the reduction in flow velocity across the surface. Consequently, it can be seen that the values of the corrections estimated for this effect agree reasonably well with the discrepancies between the observed and computed results. It is likely that these flow conditions are the major factor causing the discrepancies.

Corrections were made to allow for the combined effects of the lateral flow and pressure fluctuations on the efficiency of operation of the model openings, and using these values approximate estimates of corrected ventilation rates and internal pressures were made. The corrected ventilation rates agreed well with the observed values, the average error between corresponding values for all sets of results being approx 3%. The corrections to the ventilation rates calculated for the 1·0 mm dia openings in boundary layer I were the smallest in value; the mean ventilation rate being 0·97 for angles of incidence between 0 and 60°, while the observed value was 0·98. The largest corrections were calculated for 2·5 mm dia openings in boundary layer II; the mean value of corrected ventilation rate being 0·83 of the computed ventilation rate, while the observed value was 0·81. The pressure difference ratios showed less good agreement. Values calculated for the 2·5 mm openings agreed quite well with the observed values, but the values calculated for the 1·0 mm dia openings were lower than the observed values. In all cases however the corrections indicated that larger pressure drops would be expected to occur across the windward face, due to reduced efficiency of operation of those openings, as was observed in the model experiments. Consequently, the combined effect of these two factors was taken to be a reasonable explanation for the discrepancies noted between the observed and computed results.

In addition to the comparative model results two further small studies were carried out. In the first the ventilation rate calculations were repeated, for all the model studies carried out, using mean pressure coefficient values for the model face instead of individual values for each opening. The total ventilation rates calculated under these conditions showed close agreement with the previously calculated rates. The agreement between the two sets of ventilation rates was within 2–3% for all sets of results.

The influence of small scale surface features on ventilation rates was also investigated in order to estimate the inaccuracies caused by neglecting these features when choosing appropriate pressure coefficient values. Features such as protruding beams or columns gave variations of $\pm 7\%$ of the previously observed ventilation rates.

9. CONCLUSIONS

The results of the comparative studies of natural ventilation of a series of simple models showed that ventilation rates and pressure distributions throughout the model could not be accurately predicted using conventional natural ventilation theory. Calculated ventilation rates were higher than the observed rates; the differences between observed and predicted ventilation rates increased in more turbulent flow conditions and in the tests carried out with the larger ventilation openings. The pressure difference distributions also showed significant variation from the computed distributions. Pressure differences were larger across the windward model faces than across leeward faces. In some conditions, using the model with two identical porous faces, the pressure drop across the windward face reached $\frac{2}{3}$ of the total pressure drop across the model.

The discrepancies between the observed ventilation rates and pressure distributions and the corre-

sponding computed values were caused by reductions in the efficiency of the ventilation openings when compared to their calibrated efficiencies under conditions of steady pressure difference. The openings in the windward faces of the models were affected to a much greater extent than the openings in the leeward faces. The reductions in efficiency are thought to have been caused by fluctuations in the pressure difference acting across the openings and by lateral flow along the surfaces of the model faces. Approximate corrections allowing for these effects showed good agreement with the observed ventilation rates.

The computed ventilation rates showed discrepancies from the observed rates of 0–30%. It is possible that in full scale buildings discrepancies of this order of magnitude will also occur as the relative lateral flow velocities and pressure fluctuations will probably be of a similar order of magnitude to those experienced in the model work. The limits of accuracy of available data for predicting design wind speeds, window infiltration coefficients and pressure coefficient values is such that the digital analogue could be used to produce an acceptably accurate estimate of total full scale ventilation rates. Simplification of information requirements by using mean pressure coefficient values for the building faces, ignoring the effect of small scale surface features, did not lead to significant additional errors.

Acknowledgements—The work described in this paper was carried out while both authors were in the Department of Building Science, Sheffield University, U.K. We would therefore like to express our gratitude to the staff of that Department for their assistance during the course of the research.

REFERENCES

1. P. J. JACKMAN and H. DEN OUDEN, The natural ventilation of tall office buildings. *Research Institute for Public Health Engineering, T.N.O. Delft, Publication* 304.
2. P. J. JACKMAN, A study of natural ventilation of tall office buildings. *H.V.R.A. Lab. Rep. No.* 53 (1969).
3. E. G. SMITH, The feasibility of using models for predetermining natural ventilation, *Texas Engineering Experimental Station Research Report No.* 26 (1951).
4. B. GIVONI, Basic study of ventilation problems in hot countries. *Final Report Israel Institute of Technology, Building Research Station, Technion City* (1962).
5. E. HARRISON, The heating of buildings by off-peak electricity supplies. Appendix 2. Air infiltration into heated buildings. *J. Inst. Heat. Vent. Engrs* 33–70 (1962).
6. ANON, The assessment of wind loads. *Building Research Station Digest* 119 (1970).
7. E. R. HITCHEN and C. B. WILSON, A review of experimental techniques for the investigation of natural ventilation in buildings, *Build. Sci.* **2**, 59–83 (1967).
8. J. S. WANNERBURG and J. F. VAN STRAATEN, Wind tunnel test on scale model buildings, *J. Inst. Heat. Vent. Engrs* **24**, 477–493 (1957).
9. A. LENKEL, Close clearance orifices. *Product Engng* **36**, 57–61 (1965).
10. A. G. DAVENPORT, The dependence of wind loads on meterological parameters. *Conf. Proc. Wind Effects on Buildings and Structures, Ottawa, Canada* (1967).
11. R. E. BILSBORROW, Natural Ventilation of Buildings. Ph.D. Dissertation, University of Sheffield (1973).
12. T. V. LAWSON, Architects journal handbook of building environment, Section 3, Air movement and natural ventilation. *Architects' J.* 1283–1292 (1968).